

1 **Title**

2 A γ -Lactam Siderophore Antibiotic Effective Against Multidrug-Resistant *Pseudomonas aeruginosa*,
3 *Klebsiella pneumoniae*, and *Acinetobacter* spp.

4

5 **Affiliations**

6 ¹Research Service, Louis Stokes Cleveland Department of Veterans Affairs Medical Center,
7 Cleveland, OH 44106, USA

8 ²Department of Biochemistry, Case Western Reserve University, Cleveland, OH 44106, USA

9 ³Yale Center for Molecular Discovery, West Haven, CT 06516, USA

10 ⁴Department of Medicine, Case Western Reserve University, Cleveland, OH 44106, USA

11 ⁵Geriatric Research, Education and Clinical Center, Louis Stokes Cleveland Department of
12 Veterans Affairs Medical Center, Cleveland, OH 44106, USA

13 ⁶Department of Pathology, University Hospitals Cleveland Medical Center, Division of Clinical
14 Microbiology, Cleveland, OH 44106, USA

15 ⁷University of North Carolina School of Medicine, Chapel Hill, NC 27514, USA

16 ⁸Center for Discovery and Innovation, Hackensack Meridian Health, Nutley, NJ 07601, USA

17 ⁹Departments of Pharmacology, Molecular Biology & Microbiology, and Proteomics &
18 Bioinformatics, Case Western Reserve University, Cleveland, OH 44106, USA

19 ¹⁰CWRU-Cleveland VAMC Center for Antimicrobial Resistance and Epidemiology (Case VA
20 CARES), Cleveland, OH 44106, USA

21

22

23 **Authors**

24 Joel A. Goldberg,¹ Vijay Kumar,² Elizabeth J. Spencer,³ Denton Hoyer,³ Steven H. Marshall,¹
25 Andrea M. Hujer,^{1,4} Kristine M. Hujer,^{1,4} Christopher R. Bethel,¹ Krisztina M. Papp-Wallace,^{1,2,4}
26 Federico Perez,^{1,4,5} Michael R. Jacobs,^{4,6} David van Duin,⁷ Barry N. Kreiswirth,⁸ Focco van den
27 Akker,^{*2} Mark S. Plummer,^{*3} and Robert A. Bonomo,^{*1,2,4,5,9,10}

28

29 **Corresponding Authors**

30 Phone: 216-791-3800 x 4801. Robert.Bonomo@va.gov; marksplummer@gmail.com; Phone:
31 216-368-8511. fxv5@case.edu.

32

33 **Key Words**

34 γ -lactam

35 siderophore

36 multidrug-resistant Gram-negative pathogens

37 Penicillin-binding protein

38

39 **Abbreviations used**

40 MDR, multidrug-resistant; PBP, penicillin-binding protein; MIC, minimal inhibitory concentration; *blas*, β -
41 lactamases; SC, subcutaneously; IM, intramuscularly; CFU, colony-forming unit; WGS, whole-genome
42 sequencing; CRAB, carbapenem-resistant *Acinetobacter baumannii*; CSAB, carbapenem-susceptible
43 *Acinetobacter baumannii*; BLIs, β -lactamase inhibitors; LCMS, liquid chromatography mass
44 spectrometry; NMR, nuclear magnetic resonance; UV, ultraviolet; DMSO, dimethylsulfoxide; MSTFA, *N*-
45 methyl-*N*-(trimethylsilyl)-trifluoroacetamide; AN, *Acinetobacter nosocomialis*; FI, fluorescence intensity;
46 SAR, structure activity relationship

47

48 **Abstract**

49 Serious infections caused by multidrug-resistant (MDR) organisms (*Klebsiella pneumoniae*,
50 *Pseudomonas aeruginosa*, *Acinetobacter baumannii*) present a critical need for innovative drug
51 development. Herein, we describe the preclinical evaluation of YU253911, **2**, a novel γ -lactam
52 siderophore antibiotic with potent antimicrobial activity against MDR Gram-negative pathogens.
53 Penicillin-binding protein (PBP) 3 was shown to be a target of **2** using a binding assay with purified *P.*
54 *aeruginosa* PBP3. The specific binding interactions with *P. aeruginosa* were further characterized with a
55 high-resolution (2.0 Å) X-ray structure of the compound's acylation product in *P. aeruginosa* PBP3.
56 Compound **2** was shown to have concentration > 1 $\mu\text{g/ml}$ at the 6 hour time point when administered
57 intravenously or subcutaneously in mice. Employing a meropenem resistant strain of *P. aeruginosa*, **2**
58 was shown to have dose-dependent efficacy at 50 and 100 mg/kg q6h dosing in a mouse thigh infection
59 model. Lastly, we showed that a novel γ -lactam and β -lactamase inhibitor (BLI) combination can
60 effectively lower minimum inhibitory concentrations (MICs) against carbapenem resistant *Acinetobacter*
61 spp. that demonstrated decreased susceptibility to **2** alone.

62

63 **1. Introduction**

64 Multidrug-resistant (MDR) bacterial infections pose an increasing threat to public health, causing
65 significant morbidity, mortality, and economic hardship. In the United States alone, more than three
66 million infections each year are caused by antibiotic-resistant bacteria resulting in approximately 36,000
67 deaths and more than \$20 billion in healthcare costs [1]. The future global impact is even more
68 staggering with an estimated cumulative economic cost of \$100 trillion from now until 2050, with an
69 associated 10 million deaths, resulting from MDR infections [2]. Invasive infections with Gram-negative
70 bacterial pathogens in particular have become increasingly problematic and are associated with 28 day
71 mortality rates of 30–70% (<https://www.cdc.gov/drugresistance/biggest-threats.html>). Resistant strains
72 of *Acinetobacter baumannii*, *Pseudomonas aeruginosa*, and carbapenem-resistant Enterobacterales are
73 identified as “urgent” and “serious” threats by the CDC and WHO, illustrating the critical need for new
74 therapeutics [3-7].

75 The “hard-to-treat” nature of these infections is often caused by extensive antibiotic-resistant
76 phenotypes that allow pathogens to overcome standard antibiotic regimens [8]. Despite the increasing

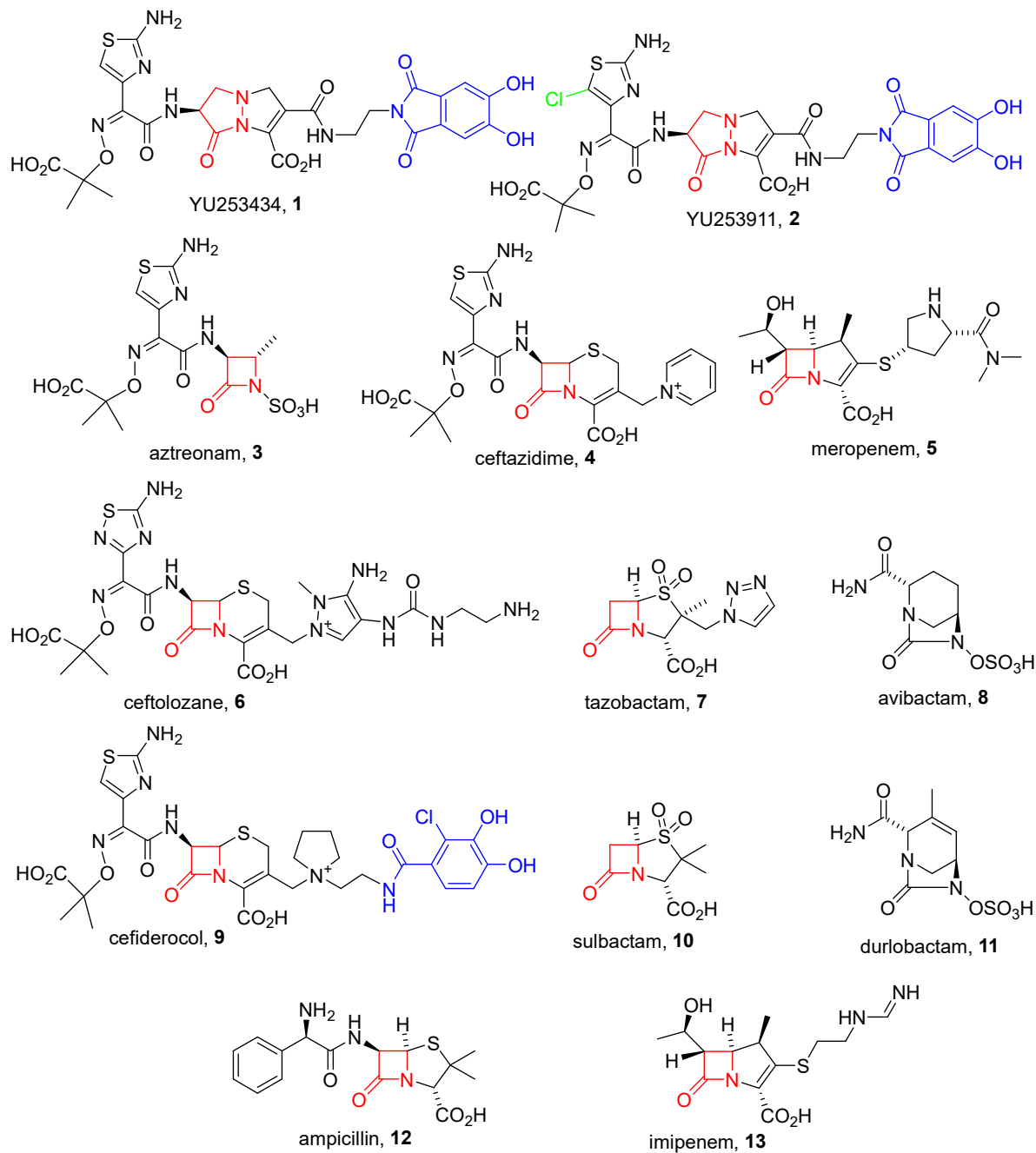
77 public health threat, few truly novel agents are in development to treat such infections, as most large
78 pharmaceutical companies have withdrawn from antibacterial research [3, 4, 9, 10]. Government
79 agencies are aware of the ever-growing issue of antibacterial resistance and are responding with several
80 initiatives intended to incentivize renewed efforts in antibiotic development [11]. They include public-
81 private partnerships highlighting the urgent need for novel treatments.

82 Resistance in multidrug-resistant Gram-negative organisms is multifactorial. These causes may include
83 reduced permeability, modification of target proteins, and overexpression of efficient and diverse efflux
84 pumps [12, 13]. For β -lactam antibiotics, a particular concern is the increasing diversity of plasmid-
85 mediated carbapenemases (β -lactamases (*blas*): NDM-1, KPC, and OXA-type class D carbapenemases)
86 making β -lactam antibiotics ineffective, despite their common coadministration with β -lactamase
87 inhibitors [1].

88 We recently reported the initial attributes of a new series of antibacterial agents effective against Gram-
89 negative pathogens based on a revitalized non- β -lactam pyrazolidinone scaffold [14 - 21] exemplified by
90 **1** (Figure 1) [22]. The strategy involves inhibiting penicillin-binding proteins (PBPs), which are validated
91 targets for antibacterial discovery, while avoiding susceptibility to β -lactamase inactivation. This is
92 accomplished by using a γ -lactam ring with tunable reactivity as the molecule's core [18, 20].
93 Additionally, **1** includes a siderophore moiety which exploits intrinsic bacterial iron transport processes
94 ("Trojan horse approach") to overcome the decreased permeability of Gram-negative bacteria [23 - 25].
95 Agent **1**, which contains a prototype γ -lactam-siderophore, inactivates PBP3 and possesses excellent *in*
96 *vitro* potency against MDR clinical isolates of *P. aeruginosa*, *K. pneumoniae*, and *E. coli*. Herein, we
97 report the discovery and properties of YU253911, **2**, a chloroaminothiazole analog of **1** (Figure 1), which
98 possesses enhanced potency versus *Acinetobacter* spp. and improved pharmacokinetics versus **1** as
99 illustrated by *in vivo* efficacy in a rodent thigh infection model employing an MDR strain of *P.*
100 *aeruginosa*.

101

102



103

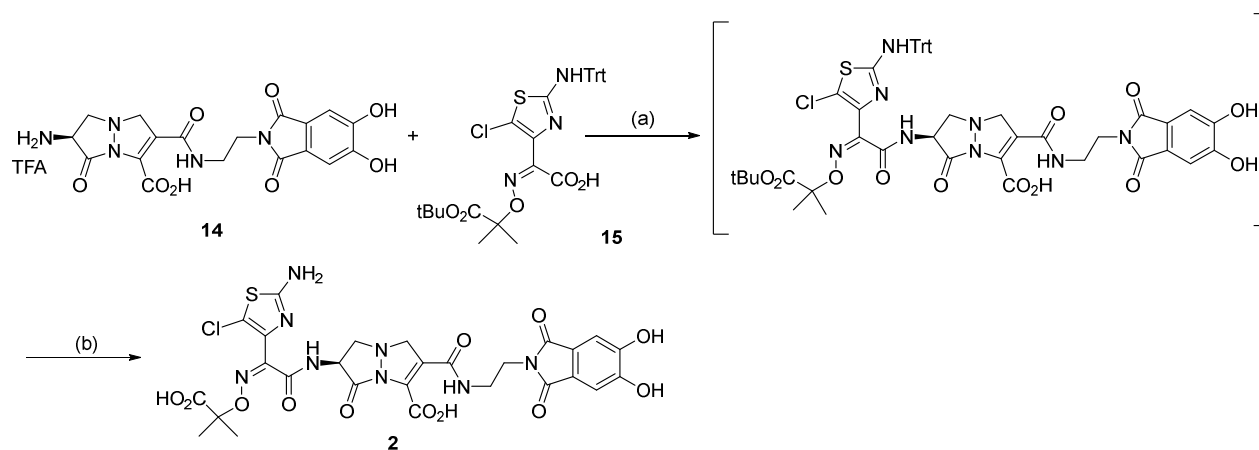
104 **Figure 1.** Structures of γ -lactam siderophores **1** and **2** versus comparator β -lactam antibiotics and β -
 105 lactamase inhibitors. The β - or γ -lactam core is highlighted in red; iron-binding siderophore moieties in
 106 blue.

107

108 **2. Results and Discussion**

109 **2.1. Chemistry**

110 We previously reported the synthesis and characterization of **1** as a prototype of a new class of
111 siderophore-conjugated γ -lactam antibiotic with enhanced activity against MDR Gram-negative bacteria
112 [22]. In an effort to explore this finding, additional analogs with modified side chains were screened,
113 leading to the identification of **2** which contains a chloroaminothiazole group. This group was found to
114 favorably modulate several biological properties (*vide infra*). The synthesis of **2** parallels the synthesis of
115 **1** and employs a common advanced intermediate dihydroxyphthalimide [26] -appended bicyclic
116 pyrazolidinone, **14** (details of the synthesis of **14** are in the Supporting Information, pages 4 -17).
117 Coupling of **14** using the appropriately protected chloroaminothiazole **15** followed by deprotection and
118 reverse phase chromatography provides compound **2**, Scheme 1. The chiral purity of **2** was not assessed
119 after the synthesis was completed though Boc-L-serine was employed as the starting material.



120

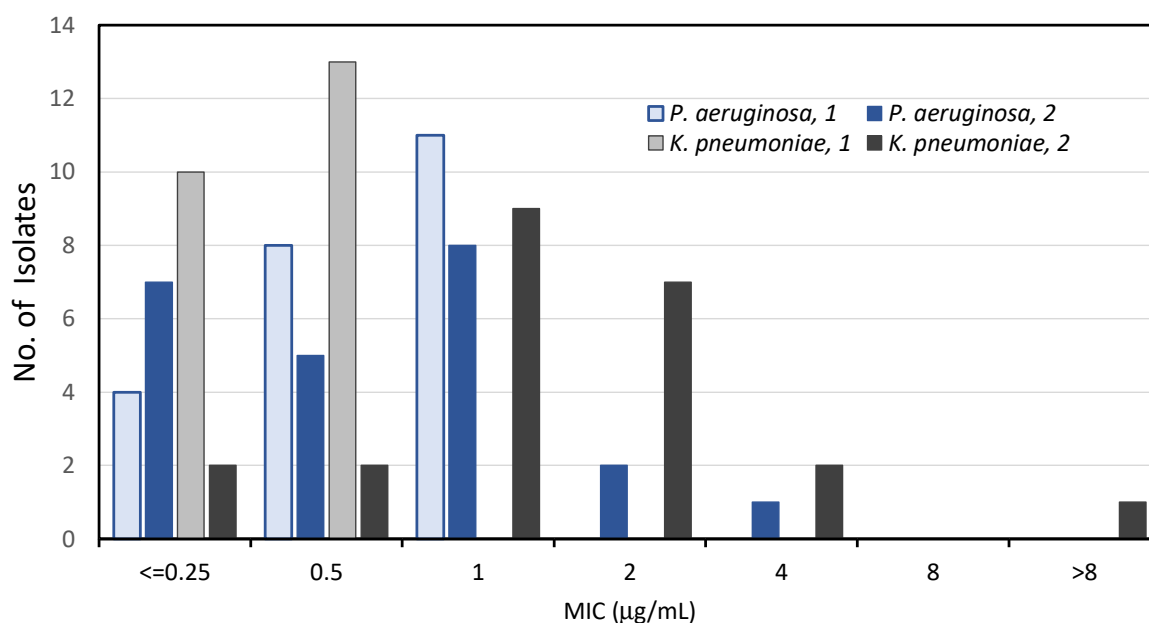
121 **Scheme 1** Synthesis of YU253911, **2**: (a) i. **15**, Oxalyl chloride, catalytic DMF; ii) **14**, MSTFA, Hunig's base,
122 3.5 h, 100% crude. (b) 2:1 DCM/TFA, triethylsilane, 0 °C to RT, 1.5 h, toluene chase, reverse phase MPLC
123 C18, 0 to 60% acetonitrile 0.1% formic acid/water with 0.1% formic acid, 30%.

124 **2.2. Microbiology**

125 **γ -Lactam **2** inhibits the growth of MDR Gram-negative bacilli.**

126 A comparison of minimum inhibitory concentrations (MICs) for **2** and **1** vs. previously described clinical
127 carbapenem-resistant isolates of *P. aeruginosa*²⁷ and *K. pneumoniae*²⁸ are provided in Figure 2 [22]. MIC
128 data for both **2** and **1** is provided for comparison; the detailed values for each individual strain are in

129 Supplemental Table 1, page 18. In all but one case (YUKP-39), microbiologic potency of **2** was
 130 maintained, although the activity trended to be slightly less active for **2** compared to **1**, particularly for
 131 *K. pneumoniae*. Nevertheless, MIC testing of **2** afforded an MIC₅₀ of 0.5 and 1 mg/mL against 23 samples
 132 each of MDR *P. aeruginosa* and *K. pneumoniae*, respectively. Notably, MIC data of **2** were significantly
 133 lower than meropenem in all cases but 1 isolate (YUKP-39). We purposely selected a subset of our *P.*
 134 *aeruginosa* and *K. pneumoniae* panels that had the most potent compound **1** MIC values. Using such a
 135 narrow comparison means it is possible that **2** may not necessarily have poorer overall activity against
 136 larger panels. Similar to what was previously reported for **1** [22], MIC values were dependent on
 137 maintaining low iron concentrations in the culture media (data not shown). All results were generated
 138 using Chelex® resin-treated media to mimic the low iron concentrations found in vivo, and in accord
 139 with CLSI recommendations for siderophore-containing antibiotics.

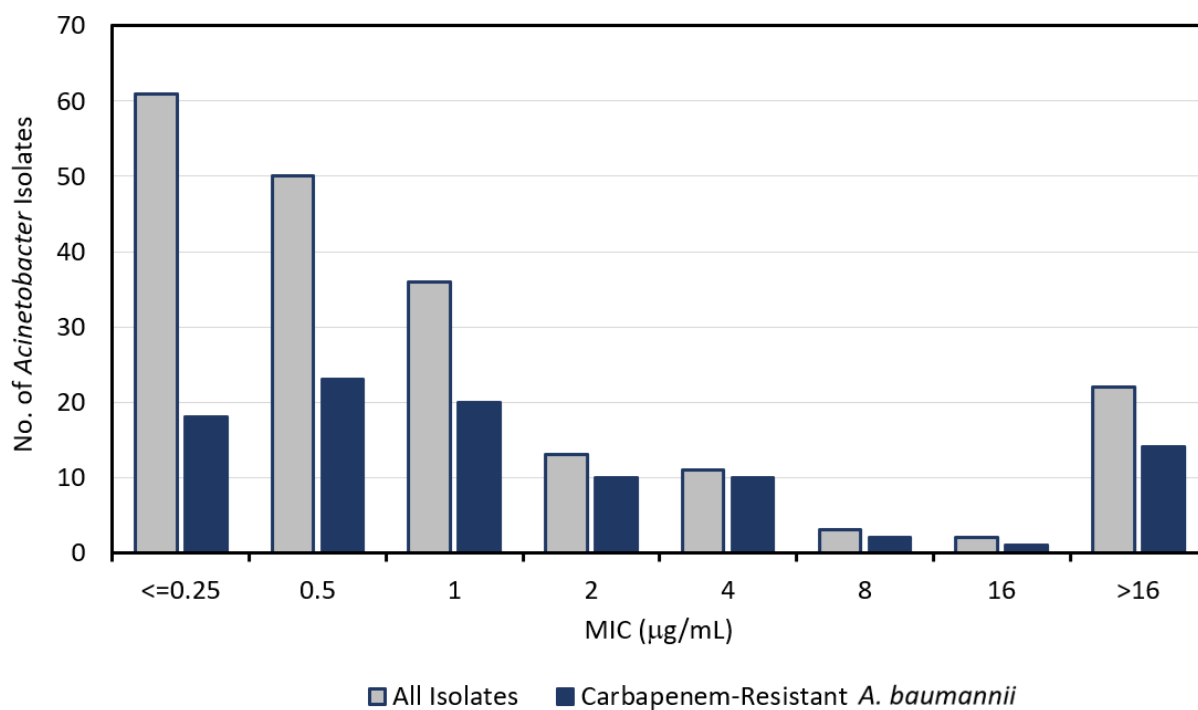


140
 141 **Figure 2.** Compound **2** and **1** MIC values against representative γ -lactam susceptible/carbapenem-
 142 resistant *K. pneumoniae* and *P. aeruginosa* strains (23 each). Except for one isolate, YUKP-39, compound
 143 **2** maintains microbiologic potency against MDR Gram-negative rods previously described for this γ -
 144 lactam-siderophore class (see also Supplemental Table 1, page 18).

145

146 **The γ -Lactam **2** possesses enhanced antimicrobial activity against MDR *A. baumannii*.**

147 MICs in low iron media against a 198-member panel of previously described *Acinetobacter* spp. clinical
 148 isolates, (79% *A. baumannii*, 21% a mixture of *A. nosocomialis*, and *A. pittii*) [30] are presented in Figure
 149 3 and Table 1. Activity against a 98-member carbapenem-resistant *A. baumannii* subset of the panel is
 150 also shown in Figure 3 and Table 1. Importantly, the MIC values of **2** compare favorably to all β -lactam
 151 classes, including aztreonam **3** (monobactam), ceftazidime **4** (cephalosporin) and meropenem **5**
 152 (carbapenem) (Table 1). Applying the breakpoints for cefiderocol **9** (susceptibility ≤ 4 $\mu\text{g/mL}$ and
 153 resistance ≥ 16 $\mu\text{g/mL}$), a similar approved drug utilizing a siderophore transport mechanism [29], to
 154 compound **2** results in a susceptibility to **2** of 86% (171 out of 198) of the full *Acinetobacter* panel and
 155 83% (81 out of 98) of the subset of carbapenem-resistant *A. baumannii* (CRAB). Detailed values for each
 156 individual strain are in Supplemental Table 2, page 19.



157
 158 **Figure 3.** Distribution of MICs in low iron media of **2** ($\mu\text{g/mL}$) against a 198-member *Acinetobacter* spp.
 159 panel and subset of 98 carbapenem-resistant *A. baumannii* (CRAB) isolates. See also Supplemental Table
 160 2, page 19.

161
 162 **Table 1.** MIC₅₀ and MIC₉₀ ($\mu\text{g/mL}$) of **2** and comparator β -lactam antibiotics against a 198-member panel
 163 of clinical isolates of *Acinetobacter* spp., as well as the 98-member subset of carbapenem-resistant *A.*

164 *baumannii* (CRAB).³⁰ Chemical structures for all agents are provided in Figure 1.^a See also Supplemental
165 Table 2, page 19.

Compound	198 <i>Acinetobacter</i> spp.		98 CRAB	
	MIC ₅₀	MIC ₉₀	MIC ₅₀	MIC ₉₀
2	0.5	>16	1	>16
Aztreonam (3)	>32	>32	>32	>32
Ceftazidime (4)	64	>64	>64	>64
Meropenem (5)	8	>64	64	>64
Ceftazidime (4)/avibactam (8)	16	>64	64	>64
Ceftolozane (6)/tazobactam (7)	8	>64	32	>64

166 ^aMICs were determined using iron-depleted cation-adjusted Mueller-Hinton broth that was
167 supplemented with iron (as ferric chloride) as indicated. The initial iron-depleted media was prepared by
168 the standard treatment with cation-exchange resin, which has been reported to reduce iron
169 concentrations to 0.02 µg/mL.²⁹

170

171 **Combination of 2 with sulbactam further enhances growth inhibition of *Acinetobacter* spp.**

172 We investigated whether partner agents could improve the already potent activity of **2** against resistant
173 *Acinetobacter* spp. growth. β-lactam antibiotics are often used clinically in combination with β-
174 lactamase inhibitors (BLIs) to protect against enzymatic hydrolysis. Although the γ-lactam core of **2**
175 possesses intrinsic stability to β-lactamase hydrolysis (*vide infra*), β-lactamase inhibitors (BLIs) were
176 nevertheless evaluated for their ability to augment the breadth of **2** susceptibility against *Acinetobacter*
177 spp.

178 Sulbactam **10**, a BLI commonly marketed in combination with ampicillin (**12**, Unasyn®), was selected for
179 study as a potential partner of **2** for two reasons. Firstly, sulbactam has been shown for decades to be
180 safe [32, 32] and well-tolerated in patients [33], with favorable pharmacokinetics [34, 35]; secondly,
181 sulbactam possesses intrinsic antimicrobial activity against *Acinetobacter* spp. due to postulated
182 inhibition of PBP1 and PBP3 [36]. Furthermore, sulbactam is currently under investigation in
183 combination with durlobactam, **11**, for the treatment of *Acinetobacter* infections. The γ-lactam **2** is
184 believed to target PBP3 (*vide infra*) and inhibition of two PBP enzymes would be expected to produce
185 enhanced antimicrobial effects.

186 The 24 *Acinetobacter* isolates from Figure 3 with higher MICs to compound **2** (MIC \geq 16 $\mu\text{g}/\text{mL}$) were
 187 tested versus sulbactam alone or in combination with **2**. MIC values show 79% (19/24) of the tested
 188 isolates were found to have their growth inhibited to some extent by sulbactam (MICs \leq 16 $\mu\text{g}/\text{mL}$)
 189 (Table 2). Furthermore, when **2** and sulbactam were combined in a 1:1 ratio in a typical 2-fold MIC
 190 dilution scheme, 50% (12/24) of the isolates previously resistant to **2** showed improved MICs \leq 4 $\mu\text{g}/\text{mL}$.
 191 Published human pharmacologic data for ampicillin-sulbactam and sulbactam-durlobactam demonstrate
 192 that serum concentrations of sulbactam of 20 $\mu\text{g}/\text{mL}$ are readily attainable from intravenous dosing.
 193 Therefore, additional studies were undertaken to evaluate the *in vitro* effectiveness of **2** under
 194 conditions of a constant level of sulbactam coadministration. The MIC values for **2** were determined
 195 using sulbactam set at 20 $\mu\text{g}/\text{mL}$ (Table 2). Under these conditions, the growth of only 3 of the isolates
 196 resistant to **2** were not significantly inhibited, collectively implying that 98% of the full 198 member
 197 *Acinetobacter* spp. panel could be susceptible to **2** when used in combination with a 20 $\mu\text{g}/\text{mL}$
 198 coadministration of sulbactam.

199

200 **Table 2.** MIC ($\mu\text{g}/\text{mL}$) values in low iron media of **2** in combination with sulbactam, **10**, when combined
 201 1:1 (by mass), or when **2** was tested with a constant concentration of **10** at 20 $\mu\text{g}/\text{mL}$. Individual MIC
 202 values for **2** and **10** are provided for comparison as well as the identity of each *Acinetobacter* isolate. See
 203 text for details.

Isolate No	Strain Identity ^a	2	10	2 + 10 (1:1)	2 + 10 (20 $\mu\text{g}/\text{mL}$)
PR-314	CRAB	>16	16	4	\leq 0.25
PR-319	CRAB	>16	>32	4	0.5
PR-325	CRAB	>16	32	>16	>16
PR-326	CRAB	>16	2	2	\leq 0.25
PR-340	CSAB	>16	4	1	\leq 0.25
PR-342	CRAB	16	>32	>16	>16
PR-345	CRAB	>16	16	16	\leq 0.25
PR-351	CRAB	>16	16	16	\leq 0.25
PR-362	AN	>16	1	\leq 0.25	\leq 0.25
PR-365	AN	>16	1	\leq 0.25	\leq 0.25
PR-380	CRAB	>16	16	16	\leq 0.25
PR-384	CRAB	>16	16	16	>16

PR-387	CRAB	>16	16	16	<=0.25
PR-399	CRAB	>16	16	16	<=0.25
PR-401	CRAB	>16	16	8	<=0.25
PR-412	AN	>16	2	1	<=0.25
PR-423	CRAB	>16	16	8	<=0.25
PR-434	CSAB	>16	8	2	<=0.25
PR-452	CSAB	>16	1	<=0.25	<=0.25
PR-459	CRAB	16	32	8	4
PR-464	CSAB	>16	1	<=0.25	<=0.25
PR-478	CSAB	16	4	1	<=0.25
PR-482	CRAB	>16	32	>16	<=0.25
PR-491	AN	>16	2	0.5	<=0.25

204 ^a Strain identity: CRAB = carbapenem-resistant *A. baumannii*; CSAB = carbapenem-susceptible *A.*
205 *baumannii*; AN = *A. nosocomialis* (carbapenem-susceptible).

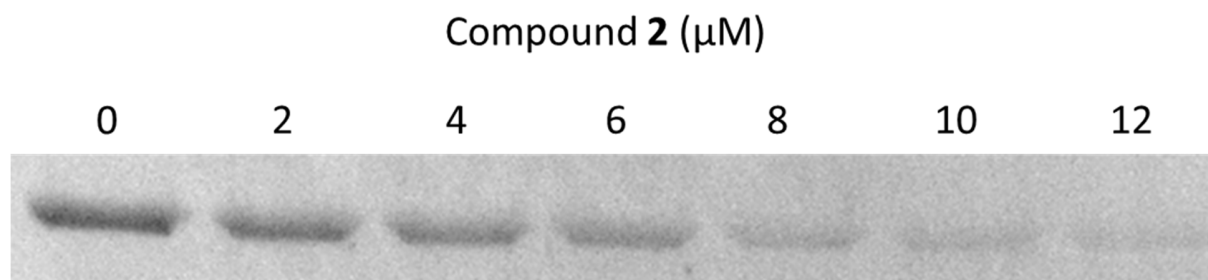
206

207

208 **2.3. PBP Inhibition**

209 Based on the mechanism established previously for γ -lactam **1**, **2** was also suspected of inhibiting PBP3,
210 an essential bacterial transpeptidase. This was verified through labeling studies with Bocillin™, a
211 fluorescent penicillin analog, using purified *P. aeruginosa* PBP3 according to an established protocol
212 [37]. Increasing concentrations of **2** inhibited fluorescent labeling of the protein by Bocillin™, with an
213 IC₅₀ of 5 ± 1 μM (Figure 4). This value is comparable to **1** (2.5 ± 0.5 μM) and a previously published value
214 for doripenem (IC₅₀ = 2.3 ± 0.5 μM, for *Acinetobacter* spp. PBP3) [37].

215

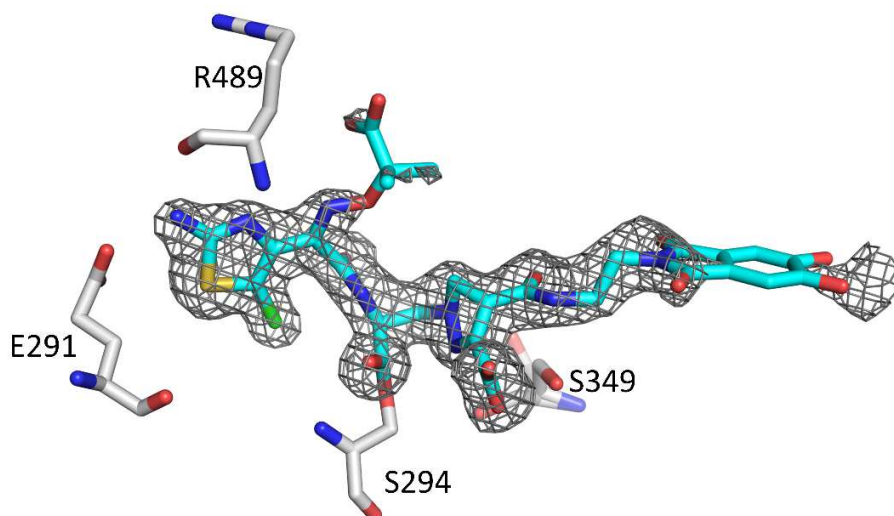


216
 217 **Figure 4.** Determination of the IC_{50} of **2** for *P. aeruginosa* PBP3 using a competitive assay. Bocillin™, a
 218 fluorescent substrate of PBP3 was reacted with enzyme that had been pre-incubated with increasing
 219 concentrations of **2**. An IC_{50} was calculated as the concentration of **2** required to reduce the
 220 fluorescence intensity of the Bocillin™-labeled protein by 50%.

221 **2.4. Crystal Structure and Molecular Modeling**

222 **The Compound 2 Crystal Structure complexed with *P. aeruginosa* PBP3a.**

223 The crystal structure of *P. aeruginosa* PBP3 complexed to **2** was determined to 2.0 Å resolution (Table
 224 3). The difference electron density in the active site shows that **2** has formed a covalent bond with the
 225 catalytic S294 residue (Figure 5). Density for most of the compound **2** moieties are well resolved. This
 226 includes the chlorine substituent on the aminothiazole ring, both amide groups, the carboxyl group and
 227 the dihydropyrazole ring of the core. Note that the occupancy for the chlorine atom refined to 0.58
 228 whereas the rest of the aminothiazole ring had an occupancy of 1.0. This decreased occupancy for the
 229 chlorine atom is likely due to radiation damage during the synchrotron radiation X-ray experiment.
 230 Halogen-aromatic ring bonds are known to be sensitive to X-ray radiation, and their breakage has been
 231 used to monitor radiation damage in protein crystals [38]. Density for the 2-carboxypropan-dimethyl
 232 moiety extending from the oxime and the 5,6-dihydroxyphthalimide siderophore group of **2** are not well
 233 resolved in the electron density map indicating their inherent flexibility (Figure 5).



234

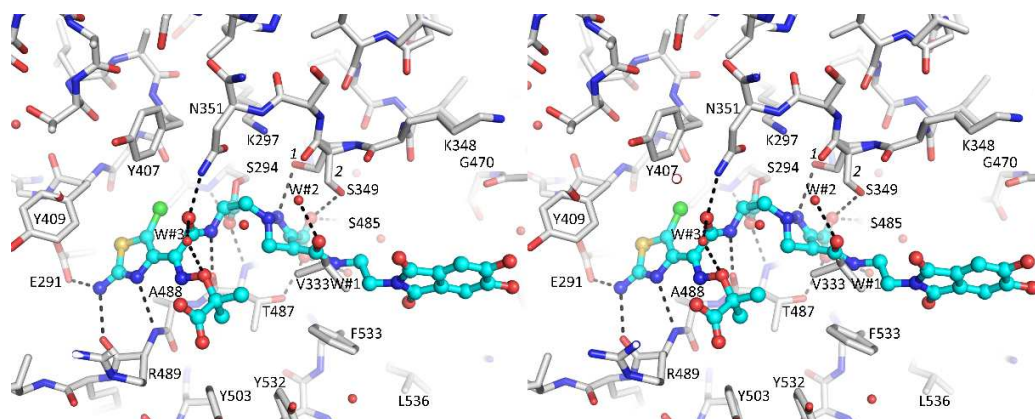
235 **Figure 5.** Omit Fo-Fc electron density showing the presence of a covalently bound **2**. The compound **2** is
 236 shown with cyan-colored carbon atoms. The density is contoured at the 3 σ level.

237

238 The ligand **2** forms a number of hydrogen bonds in the active site of *P. aeruginosa* PBP3 (Figure 6). The
 239 chloroaminothiazole ring hydrogen bonds with E291, and main chain oxygen and nitrogen atoms of
 240 R489. The chloroaminothiazole also makes hydrophobic interactions with G293, Y409, and A488. In
 241 addition, the chlorine substituent makes a special close-to-linear "C-Cl ... O" interaction with the
 242 carbonyl oxygen of Y407. Such favorable interactions with a halogen atom have previously been
 243 observed in protein:ligand interactions [39, 40]. The amide side chain, which connects to the
 244 aminothiazole ring, hydrogen bonds with N351 and the backbone oxygen of T487. The carboxyl moiety
 245 of the core hydrogen bonds with T487, S485, and conformation 2 of residue S349. The secondary
 246 nitrogen atom of the dihydropyrazole ring hydrogen bonds with conformation 1 of S349 (Figure 6). The
 247 amide moiety that serves to attach the 5,6-dihydroxyphthalimide siderophore side chain of **2** interacts
 248 with a nearby water molecule (W#2). The 5,6-dihydroxyphthalimide does not form many interactions in
 249 the active site.

250

251

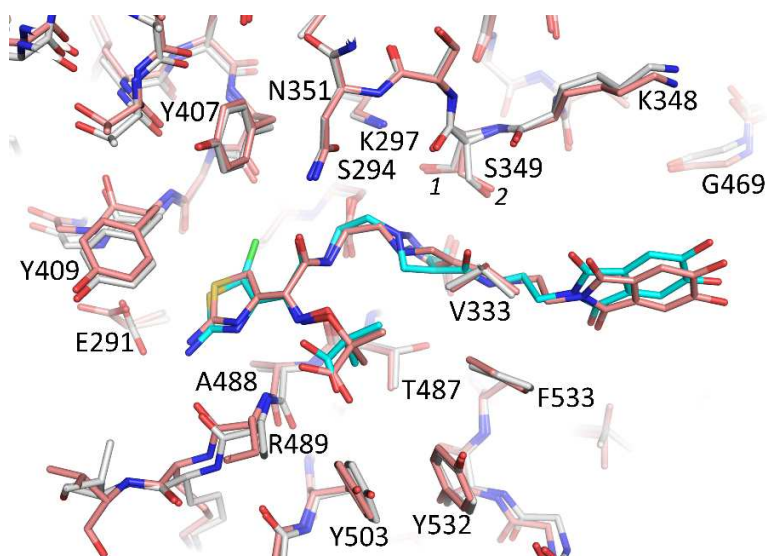


252

253 **Figure 6.** Stereo diagram depicting the interactions of **2** in the active site of *P. aeruginosa* PBP3.
 254 Hydrogen bonds are depicted as dashed lines.

255 The compound **2** is chemically identical to the previously reported **1**, except the 5-position of the
 256 aminothiazole in **2** has a chloro- substituent. The binding mode of **1** is very similar to that of **2** when
 257 bound to *P. aeruginosa* PBP3 (Figure 7; PDBid 6VOT) [22]. A difference is an inversion of the tertiary
 258 nitrogen in the dihydropyrazole ring of **2** compared to **1**. This is likely a consequence of that the **2 PBP3**
 259 complex is determined to a higher resolution (2.0 vs. 2.5 Å resolution) allowing for improved refinement
 260 of this ring region. A second difference is that residue E291 in the **2 PBP3** complex has moved closer to
 261 the aminothiazole ring compared to the **1 PBP3** complex (Figure 7).

262



263

264 **Figure 7.** Superpositioning of the **1** and **2** bound structures of *P. aeruginosa* PBP3. The carbon atoms of
265 the **1**:PBP3 complex is shown in salmon color; while **2** is colored cyan with its protein shown in white.

266 **Table 3.** X-ray diffraction data collection and crystallographic refinement statistics for the *P. aeruginosa*
267 PBP3 complex with **2**.

Wavelength (Å)	0.97946
Resolution range (Å)	50.00 - 2.00 (2.03 - 2.00)
Space group	P2 ₁ 2 ₁ 2 ₁
Unit cell (Å, °)	67.77 82.66 88.80 90 90 90
Total reflections	427,156
Unique reflections	34,157 (1,673)
Multiplicity	12.5 (12.6)
Completeness (%)	99.8 (99.8)
Mean I/sigma (I)	30.5 (4.4)
CC _{1/2}	0.995 (0.934)
R-merge (%)	15.8 (115.9)
Resolution refinement (Å)	33.91 – 2.00 (2.05 – 2.00)
Reflections used in refinement	32,335 (2,169)
Reflections used for R-free	1,770 (141)
R-work	0.174 (0.202)
R-free	0.227 (0.237)
Number of non-hydrogen atoms	3,863
Macromolecules	3,621
Ligand	49
Solvent	193
Protein residues	473
RMS(bonds, Å)	0.010
RMS(angles, °)	1.65
Ramachandran favored (%)	97.64
Ramachandran allowed (%)	2.15
Ramachandran outliers (%)	0.22

268 Statistics for the highest-resolution shell are shown in parentheses.

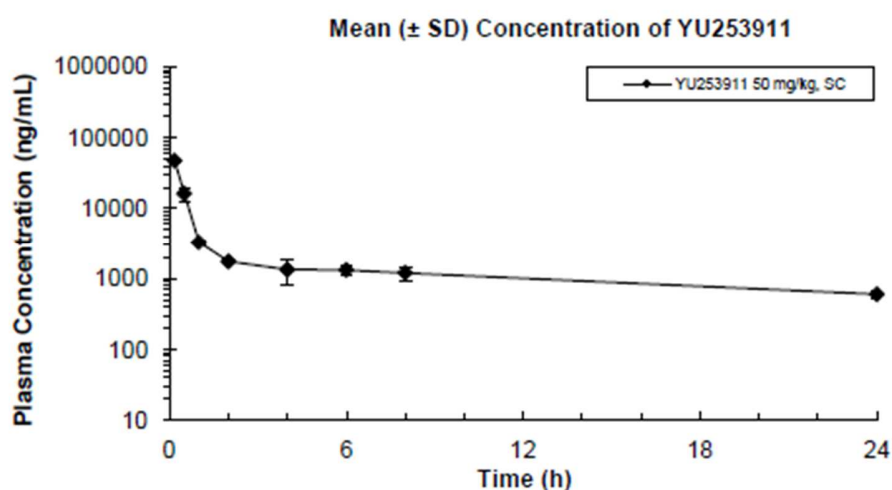
269

270 **2.5. Pharmacokinetics and In vivo efficacy; drug-like attributes**

271 Pyrazolidinone **2** has many characteristics that are favorable drug-like attributes (details of the data are
272 found in the Supporting Information, pages 33-38) for potential administration either by IV or inhaled
273 routes as **2** has high solubility >100 µM in pH 7.5 phosphate buffer as measured by nephelometry.
274 Though highly soluble, **2** has poor Caco-2 permeability and would not be expected to have oral
275 bioavailability thus IV and sub cutaneous PK was obtained (*vide infra*). Compound **2** is highly protein-

276 bound as shown by measurements in both mouse and human plasma, 94% and 88%, respectively.
277 Stability of **2** to both human and CD-1 mouse microsomes is notable with a half-life >60 minutes in both
278 preparations. Furthermore, **2** does not inhibit 7 of the 8 CYP enzymes it was tested against at a 30 μ M
279 concentration and showed approximately 50% inhibition of CYP2C8 at 100 μ M. Compound **2** was also
280 evaluated for cytotoxicity was not found when tested against human primary hepatocytes at a maximal
281 dose of 100 μ M.

282
283 In a general safety screen, testing **2** against 44 enzymes and receptors the only activity of note was >50%
284 inhibition at 30 μ M against cyclooxygenase (COX-1) and phosphodiesterase PDE3A (Supporting
285 Information, page 37). Testing against 6 ion channels, including hERG at a 30 μ M maximal dose revealed
286 **2** did not inhibit these channels (Supporting Information, page 38). The pharmacokinetics (PK) of **2** was
287 evaluated both subcutaneously and by intravenous administration at a dose of 50 mg/kg in CD-1 mice
288 (Table 4). Both routes of dosing result in similar PK data. Notably, the plasma levels of **2**, at the 6h time
289 point were >1.0 mg/mL by both dosing routes (Figure 8 and Table 4). This value is clearly superior to **1**
290 where at the 6-hour timepoint its plasma concentration was about 0.35 mg/mL [22]. The cause for
291 improved plasma level with **2** is not known, though it might be due to clearance differences caused by a
292 slight increase in protein binding or a small increase in LogP due to the additional chlorine atom.
293 Nevertheless, the >1.0 mg/mL plasma level encouraged us to comparatively test both **2** and **1** in a
294 mouse efficacy model as this plasma level is above the MIC₅₀ values of **2** for both *P. aeruginosa* and *A.*
295 *baumannii*.



296

297 **Figure 8.** The mean plasma concentration-time profile for YU253911, **2**, after sc dosing (50mg/kg) in
298 mice.

299

300

Time (h)	Sample Conc (ng/ml)			Mean (ng/ml)	SD (ng/ml)
0.167	48690	48689	44921	47433	2176
0.5	20245	14355	14094	16231	3478
1	3138	3515	3186	3280	205
2	3273	2876	3072	3074	199
4	1534	1732	739	1751	526
6	1426	1102	1425	1318	187
8	1001	1473	1126	1200	245
24	678	545	579	601	69

301 **Table 4.** Individual plasma concentrations of **2** after sc (50 mg/kg) dosing in mice, each value represents
302 an individual mouse, showing mean blood levels >1µg/mL at the 8-hour time point.

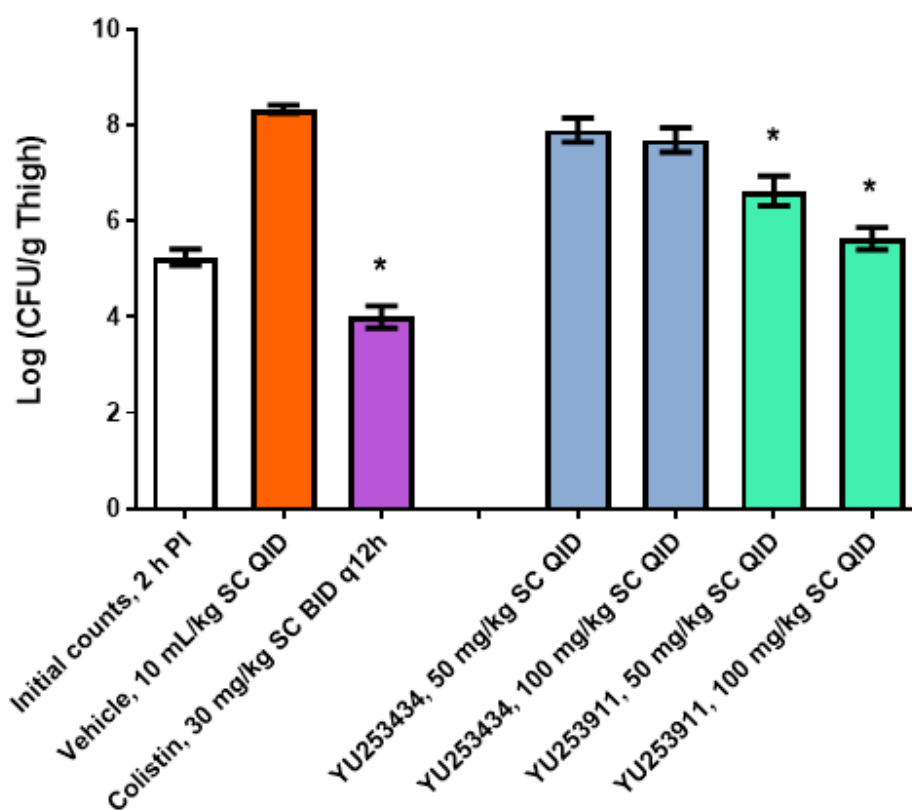
303

304 We chose AR-BANK#0229 strain of carbapenem-resistant *P. aeruginosa* as the infectious agent for the
305 neutropenic thigh infection model. This decision was made for several reasons: a) this strain establishes
306 infection in mice; b) both compound **2**, and **1** have potent activity against this strain (MIC = 0.5 µg/ml
307 and 0.25µg/mL, respectively); and c) the strain is highly resistant to currently clinically used antibiotics
308 as it is susceptible to only colistin, amikacin, and gentamicin (Supplemental Table 4, page 42).

309 Neutropenia was induced with cyclophosphamide. Animals were then intramuscularly (IM) inoculated
310 with 1.02×10^6 CFU/mouse (0.1 mL/animal) of the *P. aeruginosa* AR-BANK#0229 strain. Test antibiotics,
311 **1** and **2**, both at 50 and 100 mg/kg, were administered subcutaneously (SC) four times per day (QID)
312 with 6 h intervals (q6h) at 2, 8, 14 and 20 h after infection. The reference control was colistin, which
313 was dosed at 30 mg/kg and administered subcutaneously (SC) twice (BID) with 12 h intervals (q12h) at 2
314 and 14 h after infection. Animals were sacrificed at 2 or 26 h post-infection, and the thigh tissues were
315 harvested and weighed from each of the test animals. The bacterial counts (CFU/g) of thigh tissue
316 homogenates were compared. Full details of the method and protocol are in the Supplemental

317 Information as well as the individual animal data (Supplemental Information, pages 45-57). Bacterial
318 burden (CFU/g tissue) of test article treated animal groups was compared to the baseline bacterial count
319 at 2 h after infection and the difference in counts (Δ) was reported. The significance of effects was
320 assessed with ANOVA. The burden was also compared to the vehicle control.

321 As might have been predicted by the pharmacokinetic results, **1** was not found to have efficacy in the
322 animal model against this carbapenem-resistant strain even though the MIC values indicated the strain
323 had good susceptibility of 0.25 $\mu\text{g}/\text{mL}$ (Figure 9). Importantly, **2**, with superior pharmacokinetics does
324 show a dose-dependent reduction in CFU values against this difficult to treat *P. aeruginosa* strain. It is
325 notable that the MIC value for **2** of 0.5 $\mu\text{g}/\text{mL}$ is below the expected blood levels of **2** at the 6 hour
326 dosing interval and, in spite of the high protein binding of 94%, encouraging activity was seen (Figure 9).



327
328 **Figure 9.** The test compounds YU253434 **1**, YU253911 **2**, and colistin efficacy in the *P. aeruginosa* AR-
329 BANK#0229 thigh infection model.

330 (*) A significant difference ($p < 0.05$) between the vehicle control and treatment group was determined
331 by one-way ANOVA followed by Dunnett's test.

332 Error bars are SEM values.

333

334

335

336

337 **2.6. Resistance**

338 Although **2** showed broad coverage against a large panel of resistant clinical isolates of *Acinetobacter*
339 spp. including carbapenem-resistant *A. baumannii*, a fraction of all tested strains (24 of 198, 12%) and
340 the carbapenem-resistant subgroup (15 of 98, 15%) demonstrated MICs ≥ 16 $\mu\text{g/mL}$.

341 Understanding the mechanism or mechanisms of resistance for **2** is important as it allows the
342 optimization of partner agents or alternative dosing schedules to ameliorate potential issues. This
343 knowledge will help predict whether further strains will be susceptible and influence future clinical use,
344 as well as design and synthesis of subsequent analogs.

345 There are a number of mechanisms that have been identified for resistance to antibiotics for
346 *Acinetobacter* spp. as well as other Gram-negative pathogens. They fall into 4 general categories: 1)
347 degradation of the antibiotic (e.g., β -lactamase hydrolysis); 2) target modification (e.g., PBP mutations
348 or changes in the expression of PBP genes); 3) efflux of the antibiotic from the periplasm or cytoplasm
349 (e.g., mutations or decreased changes in expression of pump genes such as ErmAB-TolC, macA, UadeA-
350 H, mdtABC); or 4) decreased permeability of the bacterial outer membrane (e.g., TolC, OmpH, OPRD
351 genes). All of these represent potential mechanisms for resistance to **2**. Additionally, due to the
352 incorporation of the siderophore moiety as a key component of the antibiotic molecule, changes in the
353 expression of genes related to the bacterial iron transport system could also have an effect on antibiotic
354 susceptibility as was identified as a potential resistance mechanism for cefiderocol, **9** [Ito, A. et al.
355 IDWeek 2018 poster 696. <https://idsa.confex.com/idsa/2018/webprogram/Paper69661.html>].

356 **2.7. Genomic analysis for resistance genes**

357 Our initial investigation to determine the mechanism of resistance toward **2** seen in *Acinetobacter* spp.,
358 as well as *P. aeruginosa* and *K. pneumoniae*, was undertaken by comparing the genomes of susceptible

359 and resistant organisms. Using whole-genome sequencing (WGS), potential resistance genes including β -
 360 lactamases, efflux pumps, porin proteins, PBPs, and iron transport were analyzed for potential gene
 361 mutations [41] (see supplemental genomic analysis data for details). There were no identified trends in
 362 the presence of resistance genes related to β -lactamases, efflux pumps, outer membrane porins, or iron
 363 transport when comparing isolates of all analyzed species. When analyzing the PBP genes of *P.*
 364 *aeruginosa*, a mutation in the PBP3, F533L, previously identified as a gain of function mutation for β -
 365 lactam antibiotics [42, 43] may be partially responsible for resistance to **1** and **2** (Table 5). The side chain
 366 of F533 in the active site of *P. aeruginosa* PBP3 makes contacts with the γ -lactam acylation product as
 367 seen in the X-ray structure (Figure 6).

368

369 **Table 5.** MICs ($\mu\text{g}/\text{mL}$) of γ -lactams **1** and **2** against representative susceptible (MIC ≤ 4 $\mu\text{g}/\text{mL}$) and
 370 resistant (MIC ≥ 16 $\mu\text{g}/\text{mL}$) clinical isolates of *P. aeruginosa* that have been whole genome sequenced
 371 and the identity of the amino acid at position 533: phenylalanine (wild-type) or leucine (mutation shown
 372 previously to provide gain of function for β -lactam antibiotics in some resistant strains of *P. aeruginosa*).

<i>P. aeruginosa</i> ID no.	1	2	Position 533 residue
PR-545	≤ 0.25	0.5	Phenylalanine
PR-548	≤ 0.25	1	Phenylalanine
PR-567	≤ 0.25	≤ 0.25	Phenylalanine
PR-672	≤ 0.25	≤ 0.25	Phenylalanine
PR-604	≤ 0.25	≤ 0.25	Phenylalanine
PR-638	>16	0.5	Phenylalanine
PR-676	16	2	Phenylalanine
PR-503	16	16	Phenylalanine
PR-564	>16	>16	Leucine
PR-606	16	>16	Phenylalanine
PR-627	>16	>16	Leucine
PR-635	16	16	Phenylalanine
PR-636	>16	>16	Leucine
PR-651	>16	>16	Leucine
PR-668	>16	>16	Leucine
PR-673	>16	>16	Leucine

PR-677	16	16	Phenylalanine
PR-680	>16	>16	Leucine
PR-688	>16	>16	Leucine
PR-699	>16	>16	Phenylalanine

373

374

375 **2.8. β -Lactamase stability**

376 As was previously reported, the dihydroxyphthalimide siderophore mimetic side chain appended to the
377 γ -lactam core was: a) intended to impart stability against β -lactamase hydrolysis; and b) promote
378 periplasm uptake. Thus, γ -Lactam **2** was evaluated as a potential substrate against representative
379 members of all 4 Ambler classes of β -lactamases. We did not observe measurable reactions with KPC-2
380 (class A *K. pneumoniae* carbapenemase), ADC-7 (class C *Acinetobacter*-derived cephalosporinase) or
381 OXA-23 (class D oxacillinase) when tested as purified isolated enzymes. Class B metallo β -lactamases
382 NDM-1, VIM-2, and IMP-1, however, did demonstrate measurable activity (Table 6). Remarkably, the
383 calculated catalytic efficiencies, k_{cat}/K_m of 0.003-0.02 $\mu\text{M}^{-1}\text{s}^{-1}$ were orders of magnitude lower than
384 those previously determined for a comparator antibiotic (imipenem 2.7-6.7 $\mu\text{M}^{-1}\text{s}^{-1}$) [22] and similar to
385 what was previously reported for γ -lactam **1** (0.02-0.07 $\mu\text{M}^{-1}\text{s}^{-1}$) [22]. Furthermore, the observed
386 stability to purified β -lactamase enzymes correlates with the MIC data, where a relationship was not
387 noted between microbiologic activity and the presence or absence of any β -lactamase gene. See
388 Supplemental Table 3, page 27, for the full listing of the *Acinetobacter* spp. β -lactamase genes in this
389 experiment.

390 **Table 6.** Susceptibility of **2** to β -Lactamase hydrolysis^a

Metallo- β -lactamase	k_{cat} (s^{-1})	K_m (μM)	k_{cat}/K_m ($\mu\text{M}^{-1}\text{s}^{-1}$)
NDM-1	35 \pm 4	1808 \pm 200	0.020 \pm 0.002
VIM-2	54 \pm 6	4400 \pm 450	0.012 \pm 0.001
IMP-1	5 \pm 1	1490 \pm 300	0.003 \pm 0.001
KPC-2	NM	NM	NM
ADC-7	NM	NM	NM
OXA-23	NM	NM	NM

^a Steady-state reactions of **2** were monitored using purified enzymes: KPC-2, ADC-7, OXA-23, NDM-1, VIM-2, and IMP-1. Kinetic parameters provided were determined from double reciprocal plots (Supplemental Figure 2, page 44). Measurable reaction

was not detected for KPC-2, ADC-7, or OXA-23 using 200 nM enzyme concentration and 100 μ M **2**. NM = not measureable.

391 **2.9. Efflux inhibitor experiments**

392 To further investigate potential resistance mechanisms, the growth inhibition of **2** in combination with
393 efflux pump inhibitors (EPIs) was examined. The MIC (μ g/mL) values of **2** in combination with the EPIs
394 carbonyl cyanide 3-chlorophenylhydrazone (CCCP) or phenylalanine-arginine β -naphthylamide (Pa β N)
395 were tested against a subgroup of *Acinetobacter* spp. isolates resistant to **2** (Supplemental Table 4, page
396 32). The EPIs were kept at a constant concentration at levels commonly used in published reports
397 against Gram-negative bacteria (2 μ g/mL for CCCP and 32 μ g/mL for PA β N). No significant inhibition
398 effect on growth was observed directly from the EPIs, and no consistent effect on MIC values were
399 observed when combined with **2**. Potential synergistic effects were observed for only one isolate, PR-
400 452, when combined with CCCP and since this was not a general effect, a detailed investigation was not
401 pursued.

402

403 **3. Conclusions**

404 In conclusion, we demonstrate the potency and effectiveness of a novel γ -lactam siderophore antibiotic.
405 Our intent was to build upon previous investigations performed with compound **1**. We show potency
406 against MDR strains of *K. pneumoniae*, *Acinetobacter* spp., and *P. aeruginosa* (MIC₅₀ \leq 0.5 μ g/ml vs. $>$ 8
407 for meropenem). Consistent with these microbiological findings, molecular analyses reveal stability
408 against problematic β -lactamases. The atomic structure of *P. aeruginosa* PBP-3 at 2.0 Å resolution
409 revealed an important "C-Cl ... O" interaction with the carbonyl oxygen of Y407. PK/PD and animal
410 testing established that reductions in CFU were significant when compared to colistin. Importantly,
411 toxicity was not evident in a series of assays. Against CRAB, we lowered MICs significantly by combining
412 **2** with sulbactam, designing a novel γ -lactam BLI combination. Studies are planned to further increase
413 our understanding regarding optimal structure activity relationships (SARs) and dosing to overcome
414 resistant infection.

415

416 **4. Experimental**

417 **4.1. Syntheses**

418 The reagents and solvents used for synthesis were of reagent grade quality. Dry solvents were
419 purchased and used as such. All compounds were individually purified by chromatography on silica gel
420 or by recrystallization and were of >95% purity for characterization purposes as determined by LCMS
421 using UV absorption at 220 or 280 nm and/or NMR integration. In practice, compounds were not always
422 purified to >95% purity prior to using in the next synthetic step, and often crude material was of
423 sufficient purity and was carried forward. Copies of the spectra of **2** are included in the Supplemental
424 Information, page 8.

425

426 **Synthesis of (S,Z)-6-(2-(((1-(tert-butoxy)-2-methyl-1-oxopropan-2-yl)oxy)imino)-2-(5-chloro-2-**
427 **(tritylamino)thiazol-4-yl)acetamido)-2-((2-(5,6-dihydroxy-1,3-dioxoisindolin-2-yl)ethyl)carbamoyl)-5-**
428 **oxo-6,7-dihydro-1H,5H-pyrazolo[1,2-a]pyrazole-3-carboxylic acid.**

429 (Z)-2-(((1-(tert-butoxy)-2-methyl-1-oxopropan-2-yl)oxy)imino)-2-(5-chloro-2-(tritylamino)thiazol-4-
430 yl)acetic acid [44] **15** (537 mg, 0.89 mmol) in dry dichloromethane (7 mL) and catalytic DMF was cooled
431 in an ice bath and treated with oxalyl chloride (484 μ L of 2.0 M solution, 0.97 mmol) and stirred for 1
432 hour. In a second flask starting amine **14** as the TFA salt (348 mg, 0.81 mmol) in dichloromethane (7 mL)
433 was cooled in an ice bath and MSTFA (600 μ L, 3.2 mmol) and Hunig's base (773 μ L, 4.4 mmol) was
434 added. After stirring for 20 minutes all of the starting amine was in solution. During this time the
435 dichloromethane from the acid chloride forming reaction was evaporated and placed on a high vacuum
436 to give a colorless foam. This foam was dissolved in dry DCM (7 mL) and added to the MSTFA treated
437 amine followed by the addition of Hunig's base (250 μ L, 1.4 mmol). The reaction was allowed to warm
438 to room temperature over 1 hour and stirred overnight to give the crude product (S,Z)-6-(2-(((1-(tert-
439 butoxy)-2-methyl-1-oxopropan-2-yl)oxy)imino)-2-(2-(tritylamino)thiazol-4-yl)acetamido)-2-((2-(5,6-
440 dihydroxy-1,3-dioxoisindolin-2-yl)ethyl)carbamoyl)-5-oxo-6,7-dihydro-1H,5H-pyrazolo[1,2-a]pyrazole-
441 3-carboxylic acid that was not isolated but directly deprotected in situ.

442

443 **Synthesis of (S,Z)-6-(2-(2-amino-5-chlorothiazol-4-yl)-2-(((2-carboxypropan-2-yl)oxy)imino)acetamido)-**
444 **2-((2-(5,6-dihydroxy-1,3-dioxoisindolin-2-yl)ethyl)carbamoyl)-5-oxo-6,7-dihydro-1H,5H-pyrazolo[1,2-**
445 **a]pyrazole-3-carboxylic acid (**2**).**

446 To the crude material from the overnight reaction above (0.82 g, 0.81 mmol) was added triethyl silane
447 (0.64 mL, 4.0 mmol). The solution was cooled in and ice bath and trifluoroacetic acid (6.2 mL, 81 mmol)

448 was added. The ice bath was removed after 30 minutes and the reaction was stirred at room
449 temperature for 1 hour. Toluene (25 mL) was added and the reaction was evaporated to dryness. The
450 crude reaction mixture was dissolved in dimethyl sulfoxide, diluted with water and chromatographed
451 using reverse phase C18 MPLC eluting with 0 to 40% acetonitrile with 0.1% formic acid in water with
452 0.1% formic acid to give the product (S,Z)-6-(2-(2-amino-5-chlorothiazol-4-yl)-2-(((2-carboxypropan-2-
453 yl)oxy)imino)acetamido)-2-((2-(5,6-dihydroxy-1,3-dioxoisindolin-2-yl)ethyl)carbamoyl)-5-oxo-6,7-
454 dihydro-1H,5H-pyrazolo[1,2-a]pyrazole-3-carboxylic acid, **2**, as a yellow powder after lyophilization (139
455 mg, 23%). ¹H NMR (400 MHz, DMSO-*d*₆) δ 12.61 (s, 1H), 10.34 (s, 4H), 8.78 (d, *J* = 8.34 Hz, 1H), 8.56 –
456 7.91 (m, 1H), 7.38 (s, 2H), 7.12 (s, 4H), 5.03 (dt, *J* = 8.05, 10.89 Hz, 1H), 4.11 (d, *J* = 12.50 Hz, 1H), 3.81
457 (dd, *J* = 6.81, 10.26 Hz, 2H), 3.67 – 3.48 (m, 2H), 2.96 (dd, *J* = 8.71, 10.98 Hz, 1H), 1.66 – 1.36 (m, 6H).
458 Mass spectrum M+H⁺ = 721.0; HRMS (ESI/QTOF) Calcd for C₂₇H₂₅Cl₁N₈O₁₂S₁ 720.1001, found M+H⁺
459 721.1077.

460

461 **4.2. Minimum Inhibitory Concentrations, MICs**

462 Bacterial strains used were from previously described collections [22, 45]. MICs were determined using
463 the general recommendations of the Clinical and Laboratory Standards Institute (CLSI). Standard broth
464 microdilution methods were followed but with a slightly lower inoculum (6 × 10⁴ cfu/mL) which afforded
465 no difference in MICs in our testing. MICs were performed using iron-depleted cation-adjusted Mueller-
466 Hinton broth, except as mentioned elsewhere, using a standard protocol used with other siderophore-
467 containing antibiotics.

468

469 **4.3. Protein expression, purification, crystallization, and structure determination of the compound 2 P.** 470 ***aeruginosa* PBP3 complex.**

471 The *P. aeruginosa* PBP3 protein was expressed, purified, and crystallized as previously described [22]. A
472 crystal of *P. aeruginosa* PBP3 was soaked with 2 mM compound **2** for 43 hours in mother liquor before
473 freezing the crystal in liquid nitrogen prior to data collection. Data were collected at the SSRL
474 synchrotron beamline 12-2 and processed to 2.0 Å resolution using HKL3000 [46]. The structure was
475 solved using molecular replacement using PHASER [47] with the PBP3 ceftazidime complex protein
476 coordinates as the search model (PDB ID 3PBO). The structure was refined using REFMAC 5 [48], and the
477 program Coot [49] was used for model building. Refinement parameter files for compound **2** were
478 generated using ACEDRG [50]. Molecular figures were generated using Pymol (www.pymol.org). The

479 coordinates and structure factors of the *P. aeruginosa* PBP3 YU253911 complex have been deposited
480 with the Protein Data Bank (PDB ID 7LC4).

481

482 **4.4. PBP Binding Kinetics**

483 A method was adapted from the work using purified, soluble *P. aeruginosa* PBP3 and BocillinTM, a
484 fluorescent β -lactam and substrate [37]. Reactions were conducted in 10 mM phosphate-buffered saline
485 at pH 7.4 using 1.6 μ M *P. aeruginosa* PBP3 incubated with increasing concentrations of **2**. To ensure that
486 equilibrium between **2** and PBP3 occurred, the enzyme was preincubated with the compound for 20 min
487 at 37 °C before the addition of 50 μ M BocillinTM and then incubated for an additional 20 min. The
488 reactions were stopped by adding SDS-PAGE loading dye and boiling for 2 min. Samples were analyzed
489 by SDS-PAGE and the gel illuminated at $\lambda = 365$ nm and imaged with a Fotodyne gel imaging system.
490 ImageJ analysis software was used to assign fluorescence intensity (FI). The IC₅₀ was calculated as the
491 concentration of **2** required to reduce the FI of the BocillinTM-labeled protein by 50%.

492

493 **4.5. β -lactamase stability testing**

494 Steady-state kinetics were determined with purified enzymes (KPC-2, ADC-7, OXA-23, NDM-1, VIM-2,
495 and IMP-1) using an Agilent model 8453 diode array spectrophotometer as previously described [22].
496 Assays were performed at 25 °C (room temperature) using 10 mM PBS, pH 7.4 (KPC-2, ADC-7), 50 mM
497 sodium phosphate buffer supplemented with 20 mM sodium bicarbonate (OXA-23) or 10 mM HEPES, pH
498 7.5, 0.2 M NaCl, 50 μ g/ml bovine serum albumin, and 50 μ M Zn (NDM-1, VIM-2, and IMP-1).

499 Compound **2** was used as a substrate at excess molar concentrations to establish pseudo-first-
500 order kinetics. The following extinction coefficient was used: **2**, $\Delta\epsilon_{336} = -4362$ M⁻¹ cm⁻¹. For velocity
501 determinations, a 0.2 cm path length quartz cuvette was employed. Hydrolysis of 600 μ M **2** was
502 monitored over time until completion. Based on the starting absorbance ($\lambda = 336$ nm, 600 μ M **2**) and
503 final absorbance ($\lambda = 336$ nm, 0 μ M **2**), concentrations of **2** were determined along the progress curve
504 and velocities during a 10 second period for each concentration calculated. A double reciprocal plot
505 ($1/[S]$ vs. $1/V$) was employed to obtain the steady-state kinetic parameters V_{max} , k_{cat} , and K_m according to
506 Equations 1 and 2:

507

$$508 \quad 1/V = K_m/V_{max}(1/[S]) + 1/V_{max} \quad \text{Eq. 1}$$

509

510 $k_{cat} = V_{max}/[E]$ Eq. 2

511
512 where V = reaction velocity, K_m = Michaelis-Menten constant, V_{max} = maximum reaction velocity, and $[S]$
513 = substrate concentration. Compound **1** was retested with NDM-1, VIM-2, and IMP-1 using this same
514 method, resulting in similar values to those previously reported [22] (Supplemental Figure 1, page 43
515 and Supplemental Table 5, page 44).

516

517

518

519

520 **4.6. Genomic analysis**

521 *Acinetobacter* spp., and *K. pneumoniae* sequences were downloaded from the sequencing read archive
522 project PRJNA384060, PRJNA384065, and PRJNA339843, respectively (National Center for Biotechnology
523 Information, U.S. National Library of Medicine, 8600 Rockville Pike, Bethesda MD, 20894 USA).
524 *Pseudomonas aeruginosa* were sequenced by the Illumina HiSeq platform with 2x150bp paired-end
525 sequencing. Reads were assembled and annotated using PATRIC, the Pathosystems Resource
526 Integration Center [41]. Antibiotic resistant genes were identified using RES Finder (Center for Genomic
527 Epidemiology; <http://www.genomicepidemiology.org/>). Amino acid variations were identified by
528 comparison of strains to the *Acinetobacter* ATCC 17978 and ATCC 19606, *Pseudomonas aeruginosa*
529 PA01, or *Klebsiella pneumoniae* MGH 78578 (GenBank Accessions [CP000523](#), [ACQB00000000](#),
530 [CP001183](#), [CP000647](#)).

531

532

533 **References**

534 [1] a)Centers for Disease Control and Prevention (2019) Antibiotic Resistance Threats in the United
535 States, 2019 AR Threats Report <https://www.cdc.gov/drugresistance/biggest-threats.html> (accessed
536 March 11, 2020) b) Cassini, A.; Högberg, L. D; Plachouras, D.; Quattrocchi, A.; Hoxha, A.; Simonsen, G. S.;
537 Colomb-Cotinat, M.; Kretzschmar, M.E.; Devleeschauwer, B.; Cecchini, M.; Ouakrim, D. A.; Oliveira, T.
538 C.; Struelens, M. J.; Suetens, C.; Monnet, D.L.; and the Burden of AMR Collaborative Group; Attributable
539 deaths and disability-adjusted life-years caused by infections with antibiotic-resistant bacteria in the EU
540 and the European Economic Area in 2015: a population-level modelling analysis, *Lancet Infectious*
541 *Disease* **2019**, 19, 56–66. Doi: 10.1016/S1473-3099(18)30605-4.

542
543 [2] World Health Organization. *Antimicrobial Resistance: Global Report on Surveillance*, 2014.
544 <https://www.who.int/antimicrobial-resistance/publications/surveillancereport/en/> (accessed March 11,
545 2020)
546
547 [3] Spellberg, B.; Guidos, R.; Gilbert, D.; Bradley, J.; Boucher, H. W.; Scheld, W. M.; Bartlett, J. G.;
548 Edwards, J. Jr. Infectious Diseases Society of America, The epidemic of antibiotic-resistant infections: a
549 call to action for the medical community from the Infectious Diseases Society of America, *Clin. Infect.*
550 *Dis.* **2008**, 46, 155–164. Doi: 10.1086/524891.
551
552 [4] Boucher, H. W.; Talbot, G. H.; Bradley, J. S.; Edwards, J. E.; Gilbert, D.; Rice, L. B.; Scheld,
553 M.; Spellberg, B.; Bartlett, J. Bad bugs, no drugs: no ESKAPE! An update from the Infectious Diseases
554 Society of America, *Clin. Infect. Dis.* **2009**, 48, 1–12. Doi 10.1086/'5955011.
555
556 [5] World Health Organization. *Global Priority List of Antibiotic-resistant Bacteria to Guide Research,*
557 *Discovery, and Development of New Antibiotics*, 2017.
558 <https://www.who.int/medicines/publications/global-priority-list-antibiotic-resistant-bacteria/en/>
559 (accessed March 11, 2020)
560
561 [6] Peleg, A. Y.; Hooper, D. C. Hospital-acquired infections due to Gram-negative bacteria, *N. Engl. J.*
562 *Med.* **2010**, 362, 1804–1813. Doi: 10.1056/NEJMra0904124.
563
564 [7] Sydnor, E. R.; Perl, T. M. Hospital epidemiology and infection control in acute-care settings, *Clin.*
565 *Microbiol. Rev.* **2011**, 24, 141–173. Doi: 10.1128/CMR.00027-10.
566
567 [8] Hassani, M. The crisis of Gram-negative bacterial resistance: is there any hope for ESKAPE?, *Clinical*
568 *Research in Infectious Disease.* **2014**, 1, 1005–1009.
569
570 [9] Silver, L. L. Challenges of antibacterial discovery, *Clin. Microbiol. Rev.* **2011**, 24, 71–109. Doi:
571 10.1128/CMR.00030-10.
572
573 [10] Payne, D. J.; Gwynn, M. N.; Holmes, D. J.; Pompliano, D. L. Drugs for bad bugs: confronting the
574 challenges of antibacterial discovery, *Nat. Rev. Drug Discov.* **2007**, 6, 29–40. Doi: 10.1038/nrd2201.
575
576 [11] So, A. D.; Gupta, N.; Brahmachari, S. K.; Chopra, I.; Munos, B.; Nathan, C.; Outtersson, K.; Paccaud, J.
577 P.; Payne, D. J.; Peeling, R. W.; Spigelman, M.; Weigelt, J. Towards new business models for R&D for
578 novel antibiotics, *Drug Resist. Updat.* **2011**, 14, 88–94. Doi: 10.1016/j.drug.2011.01.006.
579
580 [12] Livermore, D. M. Multiple mechanisms of antimicrobial resistance in *Pseudomonas aeruginosa*: our
581 worst nightmare? *Clin. Infect. Dis.* **2002**, 34, 634–640. Doi: 10.1086/338782.
582
583 [13] Tomas, M.; Doumith, M.; Warner, M.; Turton, J. F.; Beceiro, A.; Bou, G.; Livermore, D. M.;
584 Woodford, N. Efflux pumps, OprD porin, AmpC beta-lactamase, and multiresistance in *Pseudomonas*
585 *aeruginosa* isolates from cystic fibrosis patients, *Antimicrob. Agents Chemother.* **2010**, 54, 2219–2224.
586 Doi: 10.1128/AAC.00816-09.
587
588 [14] Ternansky, R.J.; Draheim, S.E. [4.3.0] Pyrazolidionones as potential antibacterial agents, *Tet. Let.*
589 **1988**, 29, 6569–6572.

590
591 [15] Allen, N. E.; Hobbs, J. N. Jr.; Preston, D. A.; Turner, J. R.; Wu, C. Y. Antibacterial properties of the
592 bicyclic pyrazolidinones, *J. Antibiot. (Tokyo)*. **1990**, 43, 92–99. Doi: 10.7164/antibiotics.43.92.
593
594 [16] Ternansky, R. J.; Draheim, S. E. Structure-activity relationship within a series of pyrazolidinone
595 antibacterial agents. 1. Effect of nuclear modification on in vitro activity, *J. Med. Chem.* **1993**, 36, 3219–
596 3223. Doi: 10.1021/jm00074a001.
597
598 [17] Ternansky, R. J.; Draheim, S. E.; Pike, A. J., Counter, F. T.; Eudaly, J. A.; Kasher, J. S. Structure-activity
599 relationship within a series of pyrazolidinone antibacterial agents. 2 Effect of side-chain modification on
600 in vitro activity and pharmacokinetic parameters, *J. Med. Chem.* **1993**, 36, 3224–3229. Doi:
601 10.1021/jm00074a002.
602
603 [18] Boyd, D. B. Application of the hypersurface iterative projection method to bicyclic pyrazolidinone
604 antibacterial agents, *J. Med. Chem.* **1993**, 36, 1443–1449. Doi: 10.1021/jm00062a017.
605
606 [19] Jungheim, L. N.; Sigmund, S. K.; Fisher, J. W. Bicyclic Pyrazolidinones, a New Class of Antibacterial
607 Agents Based on the β -Lactam Model., *Tetrahedron Letters*, **1987**, 28, 285-288.
608
609 [20] Jungheim, L. N.; Sigmund, S. K.; Jones, N. D.; Swartzendruber, J. Bicyclic Pyrazolidinones, Steric and
610 Electronic Effects on Antibacterial Activity *Tetrahedron Letters*, **1987**, 28, 289-292.
611
612 [21] L. N. Jungheim, L.N.; Ternansky, R. J.; Holmes, R. E. Bicyclic Pyrazolidinone Antibacterial Agents
613 *Drugs of the Future*, 1990, 15, 149; Doi: 10.1358/dof.1990.015.02.114554.
614
615 [22] Goldberg, J. A.; Nguyen, H.; Kumar, V.; Spencer, E. J.; Hoyer, D.; Marshall, E. K.; Cmolik, A.; O’Shea,
616 M.; Marshall, S. H.; Hujer, A. M.; Hujer, K. M.; Rudin, S. D.; Domitrovic, T. N.; Bethel, C. R.; Papp-
617 Wallace, K. M.; Logan, L. K.; Perez, F.; Jacobs, M. R.; van Duin, D.; Kreiswirth, B. M.; Bonomo, R. A.;
618 Plummer, M. S.; van den Akker, F. A γ -Lactam Siderophore Antibiotic Effective against Multidrug-
619 Resistant Gram-Negative Bacilli *Journal of Medicinal Chemistry* **2020**, 63 (11), 5990-6002. Doi:
620 10.1021/acs.jmedchem.0c00255.
621
622 [23] Cornelis, P.; Matthijs, S.; Van Oeffelen, L. Iron uptake regulation in *Pseudomonas aeruginosa*
623 *Biometals* **2009**, 22, 15–22. Doi: 10.1007/s10534-008-9193-0.
624
625 [24] a) Wilson, B. R.; Bogdan, A. R.; Miyazawa, M.; Hashimoto, K.; Tsuji, Y. Siderophores in iron
626 metabolism: from mechanism to therapy potential trends in molecular medicine **2016**, 22,12. 1077-
627 1090. b) Schalk, I.J.; Mislin, G.L.A.; Bacterial iron uptake pathways: gates for the import of bactericide
628 compounds, *J. Med. Chem.* **2017**, 60, 4573–4576. Doi: 10.1021/acs.jmedchem.7b00554.
629
630 [25] Luscher, A.; Moynie, I.; Auguste, P.S.; Bumann, D.; Mazza, L.; Pletzer, d.; Naismith, J.H.; Kohler, T.
631 TonB-Dependant receptor repertoire of *Pseudomonas aeruginosa* for uptake of siderophore-drug
632 conjugates, *Antimicrob. Agents Chemother.* **2018**, 63, 6, e00097–e00118. Doi: 10.1128/AAC.00097-18.
633
634 [26] Baudart, M. G.; Hennequin, L.F. Synthesis and biological activity of C-3’ ortho dihydroxyphthalimido
635 cephalosporins, *The Journal of Antibiotics* **1993**, 46, 9, 1458-1470. Doi: 10.7164/antibiotics.46.1458.
636
637 [27] Evans, S. R.; Tran, T. T. T.; Hujer, A. M.; Hill, C. B.; Hujer, K. M.; Mediavilla, J. R.; Manca, C.;
638 Domitrovic, T. N.; Perez, F.; Farmer, M.; Pitzer, K. M.; Wilson, B. M.; Kreiswirth, B. N.; Patel, R.; Jacobs,
639

630 M. R.; Chem, L.; Fowler, V. G.; Chambers, H. F.; Bonomo, R. A. Rapid molecular diagnostics to inform
631 empiric use of Ceftazidime/Avibactam and Ceftolozane/Tazobactam against *Pseudomonas aeruginosa*:
632 PRIMERS IV. *Clin. Infect. Dis.* **2019**, *68*, 1823–1830. Doi: 10.1093/cid/ciy801.

633 [28] Henig, O.; Cober, E.; Richter, S. S.; Perez, F.; Salata, R. A.; Kalayjian, R. C.; Watkins, R. R.; Marshall, S.;
634 Rudin, S. D.; Domitrovic, T. N.; Hujer, A. M.; Hujer, K. M.; Doi, Y.; Evans, S.; Fowler, V. G. Jr.; Bonomo, R.
635 A.; van Duin, D.; Kaye, K. S. A prospective observational study of the epidemiology, management, and
636 outcomes of skin and soft tissue infections due to carbapenem-resistant Enterobacteriaceae. *Open*
637 *Forum Infect Dis* **2017**, *4*, ofx157. Doi: 10.1093/ofid/ofx157.

638 [29] Ito, A.; Nishikawa, T.; Matsumoto, S.; Yoshizawa, H.; Sato, T.; Nakamura, R.; Tsuji, M.; Yamano, Y.
639 Siderophore cephalosporin Cefiderocol utilizes ferric iron transporter systems for antibacterial activity
640 against *Pseudomonas aeruginosa*, *Antimicrob. Agents Chemother.* **2016**, *60*, 7396–7401. Doi:
641 10.1128/AAC.01405-16.

642 [30] Evans, S. R.; Hujer, A. M.; Jiang, H.; Hill, C. B.; Hujer, K. M.; Mediavilla, J. R.; Manca, C.; T. Tran, T. T.;
643 Domitrovic, T. N.; Higgins, P. G.; Seifert, H.; Kreiswirth, B. N.; Patel, R.; Jacobs, M. R.; Chen, L.; Sampath,
644 R.; Hall, T.; Marzan, C.; Fowler, V. G.; Chambers, H. F.; Bonomo, R. A. Antibacterial Resistance Leadership
645 Group. Informing antibiotic treatment decisions: evaluating rapid molecular diagnostics to identify
646 susceptibility and resistance to carbapenems against *Acinetobacter* spp. in PRIMERS III. *J. Clin. Microbiol.*
647 **2017**, *55*, 134–144. Doi: 10.1128/JCM.01524-16.

648 [31] Nechifor, M.; Buic, D.; Diaconu, E.; Poiata, A.; Teslariu, E.; Filip, C.; Negru, A.; Antonescu, C.
649 Pharmacological studies of sulbactam and its association with semisynthetic beta-lactam antibiotics.
650 *Rev. Med. Chir. Soc. Med. Nat. Iasi.* **1992**, *96*, 51-55.

651 [32] Berezhinskaia, V. V.; Dolgova, G. V.; Egorenko, G. G.; Svinogeeva, T. P.; Shtegel'man, L. A.; Smolkina,
652 T. V.; Nikitin, A. V. Study of general toxic and organotropic properties of ampicillin combined with
653 sulbactam. *Antibiot. Khimioter.* **1992**, *37*, 25-28. Doi: 10.1517/17425250903145251.

654 [33] Betrosian, A. P.; Douzinas, E. E. Ampicillin-sulbactam: an update on the use of parenteral and oral
655 forms in bacterial infections. *Expert Opin. Drug Metab. Toxicol.* **2009**, *5*, 1099-1112.

656 [34] Benson, J. M.; Nahata, M. C. Sulbactam/ampicillin, a new beta-lactamase inhibitor/beta-lactam
657 antibiotic combination. *Drug Intell. Clin. Pharm.* **1988**, *22*, 534-541. Doi: 10.1177/106002808802200702.

658 [35] Hampel, B.; Lode, H.; Bruckner, G.; Koeppe, P. Comparative pharmacokinetics of sulbactam/ampicillin
659 and clavulanic acid/amoxicillin in human volunteers. *Drugs.* **1988**, *35*, 29-33. Doi: 10.2165/00003495-
660 198800357-00007.

661 [36] Penwell, W. F.; Shapiro, A. B.; Giacobbe, R. A.; Gu, R. F.; Gao, N.; Thresher, J.; McLaughlin, R. E.;
662 Huband, M. D.; DeJonge, B. L. M.; Ehmann, D. E.; Miller, A. A. Molecular mechanisms of sulbactam
663 antibacterial activity and resistance determinants in *Acinetobacter baumannii*. *Antimicrob. Agents*
664 *Chemother.* **2015**, *59*, 1680-1689. Doi: 10.1128/AAC.04808-14.

665 [37] Papp-Wallace, K. M.; Senkfor, B.; Gatta, J.; Chai, W.; Taracila, M. A.; Shanmugasundaram, V.; Han,
666 S.; Zaniewski, R. P.; Lacey, B. M.; Tomaras, A. P.; Skalweit, M. J.; Harris, M. E.; Rice, L. B.; Buynak, J. D.;
667 Bonomo, R. A. Early insights into the interactions of different β -lactam antibiotics and β -lactamase

668 inhibitors against soluble forms of *Acinetobacter baumannii* PBP1a and *Acinetobacter* sp. PBP3.
669 *Antimicrob. Agents Chemother.* **2012**, *56*, 5687–5692. Doi: 1128/AAC.01027-12.

670 [38] Polsinelli, I.; Savko, M.; Rouanet-Mehouas, C.; Ciccone, L.; Nencetti, S.; Orlandini, E.; Stura, E. A.;
671 Shepard, W. Comparison of helical scan and standard rotation methods in single-crystal X-ray data
672 collection strategies *J. Synchrotron Radiat.* **2017** Jan 1, *24*(Pt 1),42-52. Doi:
673 10.1107/S1600577516018488.

674 [39] Bissantz, C.; Kuhn, B.; Stahl, M. A medicinal chemist's guide to molecular interactions *J Med*
675 *Chem.* **2010**, *53*(14), 5061-84. Doi: 10.1021/jm100112j.

676 [40] Shinda, N. K.; de Brevern, A. G.; Schmidtke, P. Halogens in Protein-Ligand Binding Mechanism: A
677 Structural Perspective *J Med Chem.* **2019**, *62*(21), 9341-9356. Doi: 10.1021/acs.jmedchem.8b01453.

678 [41] Davis, J. J.; Wattam, A. R.; Aziz, R. K.; 4,5, Brettin, T.; Butler, R.; Butler, R. M.; Chlenski, P.; Conrad,
679 N.; Dickerman, A.; Dietrich, E. M.; Gabbard, J. L.; Gerdes, S.; Guard, A.; Kenyon, R. W.; Machi, D.; Mao,
680 C.; Murphy-Olson, D.; Nguyen, M.; Nordberg, E. K.; Olsen, G. J.; Olson, R. D.; Overbeek, J. C.; Overbeek,
681 R.; Parrello, B.; Pusch, G. D.; Shukla, M.; Thomas, C.; VanOeffelen, M.; Vonstein, V.; Warren, A. S.; Xia, F.;
682 Xie, D.; Yoo, H.; Stevens, R. The PATRIC Bioinformatics Resource Center: expanding data and analysis
683 capabilities. *Nucleic Acids Res.* **2020**, *48*, 606-612. Doi: 10.1039/nar/gkz943.

684 [42] Han, S.; Zaniewski, R. P.; Marr, E. S.; Lacey, B. M.; Tomaras, A. P.; Evdokimov, A.; J. Miller, R.;
685 Shanmugasundaram, V. Structural basis for effectiveness of siderophoreconjugated monocarbams
686 against clinically relevant strains of *Pseudomonas aeruginosa*. *PNAS* **2010**, *107*, 22002-22007. Doi:
687 10.1073/pnas/1013092107.

688 [43] López-Causapé, C.; Cabot, G.; del Barrio-Tofiño, E.; Oliver, A. The versatile mutational resistome of
689 *Pseudomonas aeruginosa*. *Frontiers in Microbiology* **2018**, *9*, 1-9. Doi: 10.3389/fmicb.2018.00685.

690 [44] Preparation of siderophore conjugated pyrazolidinones, and analogs thereof as antibacterial agents;
691 Plummer, M.; Hoyer, D.; Spencer, E.; WO2020018929.

692 [45] Evans, S. R.; Hujer, A. M.; Jiang, H.; Hill, C. B.; Hujer, K. M.; Mediavilla, J. R.; Manca, C.; Tran, T. T.;
693 Domitrovic, T. N.; Higgins, P. G.; Seifert, H.; Kreiswirth, B. N.; Patel, R.; Jacobs, M. R.; Chen, L.; Sampath,
694 R.; Hall, T.; Marzan, C.; Fowler Jr, V. G.; Chambers, H. F.; Bonomo, R. A. Informing antibiotic treatment
695 decisions: evaluating rapid molecular diagnostics to identify susceptibility and resistance to
696 carbapenems against *Acinetobacter* spp. in PRIMERS III. *J Clin Microbiol* **2016**, *55*, 134-144. Doi:
697 10.1128/JCM.01524-16.

698 [46] Wladek, M.; Cymborowski, M.; Zbyszek, O.; Chruszcz, M. HKL-3000: the integration of data
699 reduction and structure solution--from diffraction images to an initial model in minutes *Acta Crystallogr*
700 *D Biol Crystallogr.* 2006 Aug;62(Pt 8):859-66. Doi: 10.1107/S0907444906019949.

701
702 [47] McCoy, A. J.; Grosse-Kunstleve, R. W.; Adams, P. D.; Winn, M. D.; Storoni, L. C.; Read, R. J. Phaser
703 crystallographic software, *J Appl Crystallogr.* **2007**, *40*, 658-674. Doi: 10.1107/S0021889807021206.

704
705 [48] Murshudov, G. N.; Skubak, P.; Lebedev, A. A.; Pannu, N. S.; Steiner, R. A.; Nicholls, R. A.; Winn, M.
706 D.; Long, F.; Vagin, A. A. (2011) REFMAC5 for the refinement of macromolecular crystal structures, *Acta*

707 *crystallographica Section D, Biological crystallography*. **2011**, 67, 355-367. Doi:
708 10.1107/S0907444911001314.

709
710 [49] Emsley, P.; Cowtan, K. C. COOT: model-building tools for molecular graphics, *Acta crystallographica*
711 *Section D, Biological crystallography*. **2004**, 60, 2126-2132. Doi: 10.1107/S0907444904019158.

712
713 [50] Long, F.; Nicholls, R.A.; Emsley, P.; Graeulis, S.; Merkys, A.; Vaitkus, A.; Murshudov, G.N. AceDRG: a
714 stereochemical description generator for ligands. *Acta Crystallogr D Struct Biol*. 2017 Feb 1;73(Pt 2):112-
715 122. Doi: 10.1107/S2059798317000067.

716

717

718 **Accession codes**

719 PDB code for *P. aeruginosa* PBP3 with bound YU253911, **2**, is PDB ID 7LC4. Authors will release the
720 atomic coordinates upon article publication.

721

722 **Acknowledgements**

723 MSP: Financial support was provided by the Program in Innovative Therapeutics for Connecticut's Health
724 grant by the Connecticut Bioscience Innovation Fund, administered by the Connecticut Innovations.

725 RAB: Research reported in this publication was supported by the National Institute of Allergy and
726 Infectious Diseases of the National Institutes of Health (NIH) under Award Numbers R01AI100560,
727 R01AI063517, and R01AI072219. This study was also supported in part by funds and/or facilities
728 provided by the Cleveland Department of Veterans Affairs, Award Numbers 1I01BX002872 to KMP-W
729 and 1I01BX001974 to RAB, from the Biomedical Laboratory Research & Development Service of the VA
730 Office of Research and Development, and the Geriatric Research Education and Clinical Center VISN 10
731 (RAB). The content is solely the responsibility of the authors and does not necessarily represent the
732 official views of the NIH or the Department of Veterans Affairs.

733 BNK: Research reported in this publication was supported by a grant from the National Institutes of
734 Health, R01AI090155.

735 RAB wishes to gratefully thank the Antimicrobial Resistance Leadership Group (ARLG) for the use of the
736 isolates. The research described in this publication is supported, at least in part, by a grant from the
737 National Institutes of Health through Duke University and the findings, opinions, and recommendations
738 expressed herein are those of the authors and not necessarily those of Duke University or the National
739 Institutes of Health. This study is also supported by the National Institute of Allergy and Infectious
740 Diseases of the National Institutes of Health (NIH) under Award Number UM1AI104681.

741 FVDA: We also thank Stanford Synchrotron Radiation Lightsource (SSRL) for help with data collection.
742 Use of the SSRL, SLAC National Accelerator Laboratory, is supported by the U.S. Department of Energy,
743 Office of Science, Office of Basic Energy Sciences under Contract No. DE-AC02-76SF00515. The SSRL
744 Structural Molecular Biology Program is supported by the DOE Office of Biological and Environmental
745 Research, and by the National Institutes of Health, National Institute of General Medical Sciences
746 (including P41GM103393). The contents of this publication are solely the responsibility of the authors
747 and do not necessarily represent the official views of NIGMS or NIH.

748

749

750

751

752

753